Development 138, 3657-3666 (2011) doi:10.1242/dev.068858

Effective fiber hypertrophy in satellite cell-depleted skeletal muscle

John J. McCarthy[1], Jyothi Mula[2], Mitsunori Miyazaki[1], Rod Erfani[2], Kelcye Garrison[2], Amreen B. Farooqui[2], Ratchakrit Srikuea[1], Benjamin A. Lawson[1], Barry Grimes[3], Charles Keller[4], Gary Van Zant[3], Kenneth S. Campbell[1], Karyn A. Esser[1], Esther E. Dupont-Versteegden[2] and Charlotte A. Peterson[2,*]

SUMMARY

An important unresolved question in skeletal muscle plasticity is whether satellite cells are necessary for muscle fiber hypertrophy. To address this issue, a novel mouse strain (Pax7-DTA) was created which enabled the conditional ablation of >90% of satellite cells in mature skeletal muscle following tamoxifen administration. To test the hypothesis that satellite cells are necessary for skeletal muscle hypertrophy, the plantaris muscle of adult Pax7-DTA mice was subjected to mechanical overload by surgical removal of the synergist muscle. Following two weeks of overload, satellite cell-depleted muscle showed the same increases in muscle mass (approximately twofold) and fiber cross-sectional area with hypertrophy as observed in the vehicle-treated group. The typical increase in myonuclei with hypertrophy was absent in satellite cell-depleted fibers, resulting in expansion of the myonuclear domain. Consistent with lack of nuclear addition to enlarged fibers, long-term BrdU labeling showed a significant reduction in the number of BrdU-positive myonuclei in satellite cell-depleted muscle compared with vehicle-treated muscle. Single fiber functional analyses showed no difference in specific force, Ca^{2+} sensitivity, rate of cross-bridge cycling and cooperativity between hypertrophied fibers from vehicle and tamoxifen-treated groups. Although a small component of the hypertrophic response, both fiber hyperplasia and regeneration were significantly blunted following satellite cell depletion, indicating a distinct requirement for satellite cells during these processes. These results provide convincing evidence that skeletal muscle fibers are capable of mounting a robust hypertrophic response to mechanical overload that is not dependent on satellite cells.

KEY WORDS: Stem cells, Growth, Adaptation, Mouse

INTRODUCTION

In the original description of satellite cells, Mauro (Mauro, 1961) showed remarkable insight when he proposed that satellite cells might have a role in skeletal muscle adaptability (Mauro, 1961). Since then, a great deal of effort has confirmed Mauro's prediction by providing a wealth of evidence showing satellite cells are involved in muscle maturation during postnatal development, regeneration from injury, hypertrophy and re-growth following atrophy (Kuang and Rudnicki, 2008; Zammit et al., 2006). Although there is a large body of literature documenting satellite cell activity during these different types of muscle plasticity, there remains no study that has directly tested the requirement of satellite cells for any of these processes. Collins and co-workers (Collins et al., 2005), however, showed, using muscle fiber grafts, that the few satellite cells associated with a single fiber were sufficient to generate over 100 new myofibers in vivo (Collins et al., 2005). The clearest evidence to date for the necessity of satellite cells for muscle growth is provided by the *Pax7* knockout mouse in which postnatal muscle growth is severely blunted as the result of a progressive depletion (~90%) of satellite cells during maturation (Oustanina et al., 2004). Not surprisingly, these same mice were incapable of mounting a normal regenerative response to muscle injury (Oustanina et al., 2004).

Unfortunately, the *Pax7*-null mouse is not a good model for determining the necessity of satellite cells in muscle growth in the adult because of severe maturation problems and high mortality (<10% survive to adulthood) (Oustanina et al., 2004; Seale et al., 2000). In addition, conclusions regarding satellite cell participation in postnatal growth cannot be extrapolated to adult muscle with confidence, as recent work has shown that satellite cells in adult muscle are intrinsically different from satellite cells at earlier periods of development as they do not require *Pax7* gene expression (Lepper et al., 2009). Historically, studies investigating the role of satellite cells in hypertrophy and re-growth have attempted to prevent satellite cell activity by blocking DNA synthesis through the use of γ-irradiation or chemical agents (Fleckman et al., 1978; Fortado and Barnett, 1985; Mitchell and Pavlath, 2001; Rosenblatt and Parry, 1992; Rosenblatt et al., 1994). Based on the results of these studies, satellite cell proliferation is currently thought to be a necessary step for mounting a robust growth response. Although the aforementioned methods are very effective at blocking cell proliferation, their utility has been questioned given the lack of cellular specificity (McCarthy and Esser, 2007). As a consequence, it is difficult to arrive at a definitive conclusion regarding the necessity of satellite cells during muscle growth. This controversy was highlighted in a published debate on whether or not satellite cell addition was obligatory for muscle hypertrophy (McCarthy and Esser, 2007;

[1]Department of Physiology, College of Medicine, University of Kentucky, Lexington, KY 40536, USA. [2]Department of Rehabilitation Sciences, College of Health Sciences, University of Kentucky, Lexington, KY 40536, USA. [3]Division of Hematology and Oncology, College of Medicine, University of Kentucky, Lexington, KY 40536, USA. [4]Department of Pediatrics, Oregon Health and Science University, Portland, OR 97239, USA.

*Author for correspondence (cpete4@uky.edu)

Accepted 20 June 2011

O'Connor and Pavlath, 2007). The final consensus reached by both parties was that more research was needed to answer definitively the question of whether or not satellite cell addition was necessary for muscle growth in the adult (O'Connor et al., 2007). Towards this end, we developed a genetic mouse model to conditionally and specifically ablate satellite cells in adult skeletal muscle to test rigorously the hypothesis that satellite cells are necessary for skeletal muscle hypertrophy.

The idea that satellite cells are required for muscle hypertrophy has been conceptually justified by the idea of myonuclear domain as first suggested by Cheek et al. (Cheek et al., 1965). The myonuclear domain theory posits that each nucleus within a muscle fiber syncytium has 'jurisdiction' over a set amount of cytoplasm. Accordingly, during periods of muscle hypertrophy, when cytoplasmic volume is increasing, the number of myonuclei per fiber increases, presumably to maintain a constant myonuclear domain (Adams et al., 2002; Bruusgaard et al., 2010; Snow, 1990; Tamaki et al., 1996). Given that myonuclei are post-mitotic, the mechanism of myonuclear accretion is thought to occur through the fusion of satellite cells to the growing myofiber, thereby contributing a nucleus (Moss and Leblond, 1970; Schiaffino et al., 1976).

To test directly the necessity of satellite cells for muscle hypertrophy, we used synergist ablation (SA) to induce hypertrophy as it provides the greatest increase in muscle mass of established animal models of muscle growth; a doubling of muscle mass within the first two weeks has been reported (Miyazaki et al., 2011; Timson, 1990). The growth response induced by SA is considered to be maximal as even the administration of an anabolic androgen failed to enhance the degree of hypertrophy (Tamaki et al., 2009a). Furthermore, it is well documented that SA induces satellite cell proliferation and the accretion of 'new', $BrdU^+$ myonuclei, presumably derived from the fusion of satellite cells (Ishido et al., 2009; Westerkamp and Gordon, 2005). Thus, if satellite cells are necessary for hypertrophy, then the growth challenge provided by SA is guaranteed to be sufficient to require satellite cells. In addition to fiber hypertrophy, the SA model has also been reported to induce both fiber hyperplasia and regeneration, providing the opportunity to assess the necessity of satellite cells in these distinct processes (Tamaki et al., 2009b).

The findings from this study indicate that satellite cells do not appear to be necessary for fiber hypertrophy but are required for both the de novo formation of new fibers and fiber regeneration. Given that the latter two processes are minor components of the overall hypertrophic response, the increase in muscle mass was no different in satellite cell-depleted muscle compared with control.

MATERIALS AND METHODS

Mice

All animal procedures were conducted in accordance with institutional guidelines for the care and use of laboratory animals as approved by the Animal Care and Use Committee of the University of Kentucky. Mice were were housed in a temperature- and humidity-controlled room and maintained on a 14:10 hour light-dark cycle with food and water ad libitum. The $Pax7^{CreER/+}$; $Rosa26^{DTA/+}$ strain, designated Pax7-DTA, was generated by crossing $Pax7^{CreER/CreER}$ and $Rosa26^{DTA/DTA}$ strains. The $Pax7^{CreER}$ strain was generated by placing an *ires-CreER*^{TM}*-FRT-Neo-FRT* cassette into the *Cla*I site of the *Pax7* gene 3′-UTR following the stop codon in exon 9 (Nishijo et al., 2009). Pax7-DTA pups were genotyped by PCR are as previously described (Nishijo et al., 2009; Wu et al., 2006).

Conditional ablation of satellite cells

Adult (4 months of age), female Pax7-DTA mice were administered by intraperitoneal (IP) injection either vehicle (15% ethanol in sunflower seed oil) or tamoxifen (2 mg/day) for five consecutive days. The IP injections were carried out two hours prior to when the lights were turned off in the room because mice become more physically active in darkness. Following a two-week washout period, vehicle and tamoxifen-treated mice were randomly divided into sham or synergist ablation (SA-2, synergist ablation for two weeks; SA-6, synergist ablation for six weeks) groups. To identify replicating satellite cells and any subsequent fusion event, mice were administered BrdU via drinking water (0.8 mg/ml) for two weeks starting immediately after the synergist ablation surgery.

Synergist ablation surgery

Surgical removal of synergist muscles (gastrocnemius and soleus) places a mechanical overload on the remaining plantaris muscle resulting in robust hypertrophy as demonstrated by a twofold change in mass within two weeks (see Fig. S1A,B in the supplementary material) (Gordon et al., 2001). Following a two-week washout period after vehicle or tamoxifen treatment, mice were subjected to either sham or synergist ablation surgery. The synergist ablation was performed as described by Tsika et al. (Tsika et al., 1995). Mice were anesthetized with an IP injection of ketamine (100 mg/kg) and xylazine (10 mg/kg). Once anesthetized and under sterile conditions, a longitudinal incision on the dorsal aspect of the lower hindlimb was made exposing the gastrocnemius muscle. The tendon of the gastrocnemius muscle was isolated and used to guide the excision of this muscle; the soleus muscle was then carefully removed without disturbing the nerve, blood supply and plantaris muscle. Upon excision, the gastrocnemius muscle was mounted, covered with a thin layer of freezing medium and then frozen in liquid nitrogen-cooled isopentane in preparation for Pax7 immunohistochemistry to determine the effectivness of satellite cell ablation. The incision was sutured and animals allowed to recover. Following two (n=6-8) or six (n=2-4) weeks, mice were anesthetized, the plantaris muscle excised and the animal euthanized by cervical dislocation. Following excision, each plantaris muscle was weighed and processed accordingly for histochemistry or single fiber function, fixed in 4% paraformaldehyde or quickly frozen in liquid nitrogen and stored at –80°C.

$BaCl_2$-induced muscle injury

Mice were anesthetized with isoflurane and the tibialis anterior (TA) injected with either 50 μl of 1.2% $BaCl_2$ solution or sterile phosphate-buffered saline (PBS). After seven days, TA muscles were collected, covered in OCT compound and frozen in liquid nitrogen-cooled isopentane. Muscle samples were sectioned (10 μm), fixed in 95% ethanol and stained with Hematoxylin and Eosin.

Immunohistochemistry and western blot reagents

Antibodies and reagents used were: anti-phospho-S6K1 (T389, cat# 9205), anti-phospho-S6K1 (T421/S424, cat# 9204), anti-Akt (cat# 9272), anti-phospho-Akt (T308, cat# 9275), anti-phospho-Akt (Ser473, cat# 9271), all from Cell Signaling Technology; anti-S6K1 (C-18, cat# sc-230, Santa Cruz Biotechnology); anti-Pax7, anti-embryonic myosin (F1.652) both from Developmental Studies Hybridoma Study Bank; anti-dystrophin (cat# VP D505); Mouse IgG Blocking Reagent (cat# MKB-2213); Vectashield mounting medium (cat# H-1000); streptavidin-FITC (cat# SA-5001); Alkaline Phosphatase (AP) Substrate Kit (cat# SK-5100), all from Vector Laboratories; anti-BrdU (cat# 11170376001, Roche); Texas Red-conjugated goat anti-mouse (cat# 610-109-121, Rockland Immunochemicals); biotinylated anti-mouse IgG (cat# 115-065-205, Jackson ImmunoResearch); Tyramide Signal Amplification (TSA) Kit (cat# T20935), DAPI (cat# D1306) both from Invitrogen; AP-conjugated goat anti-mouse IgG (cat# ab7069, Abcam).

Immunohistochemistry

Gastrocnemius or plantaris muscle was pinned to a cork block at resting length, covered with a thin layer of Tissue Tek OCT compound (Sakura Finetek) and then quickly frozen in liquid nitrogen-cooled isopentane and stored at –80°C until sectioning. Frozen muscles were sectioned (7 μm), air dried and stored at –20°C. For Pax7 detection, sections were fixed in 4% paraformaldehyde followed by epitope retrieval using sodium citrate (10 mM, pH 6.5) at 92°C for 20 minutes. Endogenous peroxidase activity was blocked with 3% hydrogen peroxide in PBS for 7 minutes followed by an additional blocking step with Mouse-on-Mouse Blocking Reagent

(Vector Laboratories). Incubation with Pax7 antibody was followed by incubation with the biotin-conjugated secondary antibody and streptavidin-HRP included within the TSA kit. TSA-Alexa Fluor 594 was used to visualize antibody-binding. DAPI (10 nM) was added briefly, then slides were washed and mounted with Vectashield fluorescent mounting media. The dystrophin antibody was applied to fresh frozen sections followed by Texas Red-conjugated goat anti-mouse secondary antibody. Sections were post-fixed in 4% paraformaldehyde and then stained with DAPI, unless BrdU detection was performed. Following dystrophin detection, sections were fixed in absolute methanol, treated with 2N HCl to denature DNA and neutralized with 0.1 M borate buffer (BORAX), pH 8.5. BrdU antibody incubation was followed by biotin-conjugated goat anti-mouse secondary antibody and streptavidin-FITC. Sections were post-fixed in paraformaldehyde and stained with DAPI. For detection of embryonic myosin heavy chain expression, sections were incubated with hybridoma supernatant F1.652 followed by AP-conjugated goat anti-mouse secondary antibody. The AP substrate kit was used for visualization followed by Hematoxylin staining of nuclei and post-fixation.

Immunohistochemistry quantification

Images were captured with a Zeiss upright microscope (AxioImager M1) and analysis carried out using the AxioVision Rel software (v4.8). To determine muscle fiber cross-sectional area, dystrophin-stained 20× magnification images were used. To capture the entire plantaris muscle cross-section required 15-20 images (700-1000 fibers for sham-operated muscle and 1000-1600 fibers for SA-2) to be analyzed. The same images used to determine cross-sectional area were used to determine the number of myonuclei per fiber. DAPI-stained nuclei that clearly resided within the muscle fiber were scored as myonuclei using the interactive measurement software. Satellite cell abundance was assessed using Pax7 staining (5× magnification) and only those loci that were scored as $Pax7^+$ by the software and were $DAPI^+$ were counted.

Myonuclear domain size

SA-2 plantaris muscle was fixed in situ at resting length by fixation in 4% paraformaldehyde for 48 hours. Single fibers were isolated by 40% NaOH digestion as described (Brack et al., 2005). Single fibers were stained with DAPI and nuclei from 15-25 fibers per animal (n=4 animals/group) within a given segment counted by z-stack analysis using the AxioImager M1 microscope. AxioVision Rel software (v4.8) was used to measure fiber segment diameter, fiber segment length, myonuclear number per fiber segment and myonuclear length.

Single fiber functional analysis

Muscle fibers were chemically permeabilized with Triton X-100 and attached to a force transducer (403, Aurora Scientific, resonant frequency 600 Hz) and a motor (312B, Aurora, step-time 0.6 mseconds). Steady-state force and tension recovery kinetics were measured as a function of the activating Ca^{2+} concentration as previously described (Campbell, 2006).

Fluorescence-activated cell sorting (FACS)

Cells were isolated by enzymatic digestion of individual gastrocnemius muscles and resuspended in PBS with 0.5% fetal bovine serum (PF buffer) as described by Hidestrand et al. (Hidestrand et al., 2008). Cells were counted, re-pelleted and resuspended in viral supernatant 2.4G2 (HB197, ATCC) at a concentration of 5×10^6 cells/ml for 15 minutes to block non-specific antibody binding. Cells were incubated with four primary antibodies: PE-anti-α7 integrin (Itga7); Alexa Fluor 647-anti-CD34; FITC-anti-CD31 (Pecam1); and APC-Alexa Fluor 750-anti-CD45 (Ptprc). Labeled cells were washed in PF buffer, filtered through a 30 μm filter and subjected to FACS analysis on a BD Biosciences FACS Aria II cell sorter equipped with lasers emitting light at 488 and 635 nm. Cell viability was >80% according to their ability to exclude propidium iodide, and only viable cells were analyzed for antibody staining. Analysis was performed at a flow rate of <5000 cells/second and data from 10,000 cells/file were obtained. Gates were set using isotype antibody controls and single-color controls. Data were analyzed using FlowJo software v7.6.

Real-time PCR

Muscles were snap frozen in liquid nitrogen and stored at –80°C. Total RNA was isolated from mouse plantaris muscle using TRIzol (Invitrogen) according to manufacturer's instructions. RNA samples were treated with TURBO DNase (Ambion) to remove genomic DNA contamination and RNA integrity was assessed using the Agilent 2100 Bioanalyzer (Agilent Technologies). First-strand cDNA synthesis from total RNA (500 ng) was performed with oligo$(dT)_{12\text{-}18}$ primer using qScript cDNA Supermix (Quanta Biosciences) according to manufacturer's instructions. The PCR reaction (21 μl) consisted of 4 μl of cDNA, 1× Perfecta SYBR Green FastMix (Quanta Biosciences) and 0.36 μM of each primer; for 18S expression cDNA was diluted 50-fold. The primers for the *Pax7* gene spanned exons 8 and 9 with a predicted T_m of ~60°C. Primer sequences and product size for each gene are as follows: *Pax7*: F=5′-GCTACCAGTACAGCCAGTATG-3′, R=5′-GTCACTAAGCATGGGTAGATG-3′, 328 bp; 18S: F=5′-TTCGGACGTCTGCCCTATCAA-3′, R=5′-ATGGTAGGCACGGCGACTA-3′. Melt curve analysis confirmed amplification of a single product for each primer set. To account for any starting difference in the amount of total RNA, *Pax7* expression was normalized to 18S expression.

Western blot analysis

To prepare total protein lysate, frozen muscle samples were homogenized in ice-cold RIPA buffer [1% Nonidet P40, 0.5% sodium deoxycholate, 0.1% SDS, 50 mM NaCl, 20 mM Tris-HCl pH 7.6, 1 mM PMSF, 5 mM benzamidine, 1 mM EDTA, 5 mM N-ethylmaleimide, 50 mM NaF, 25 mM β-glycerophosphate, 1 mM sodium orthovanadate, 10 μl/ml protease inhibitor cocktail for mammalian tissues (P8340, Sigma-Aldrich)] and protein concentration determined by the Bradford method. Protein extracts were run on SDS-PAGE gels and transferred to polyvinylidene difluoride membranes. Membranes were blocked in Odyssey Blocking Buffer (LI-COR) and then incubated with each primary antibody followed by anti-rabbit IgG (Alexa 680), visualized using the Odyssey Infrared Imaging System. Band intensity for a protein of interest was quantified using Odyssey Infrared Imaging System Application Software Version 3.0.21.

Statistical analysis

A two-factor ANOVA (vehicle/tamoxifen × sham/surgery) was performed to determine whether a significant interaction existed between factors for each dependent variable under consideration. If a significant interaction was detected, Scheffé post-hoc comparisons were performed to identify the source of significance with $P\leq0.05$.

RESULTS

Effective ablation of satellite cells in adult skeletal muscle

To test rigorously the hypothesis that satellite cells are necessary for skeletal muscle hypertrophy, we developed a genetic mouse model to conditionally ablate satellite cells in adult skeletal muscle. The satellite cell-specific driver strain ($Pax7^{CreER/CreER}$) was crossed with a strain harboring a floxed diphtheria toxin A (DTA) gene to produce the double heterozygous $Pax7^{CreER/+}$; $Rosa26^{DTA/+}$ strain, designated Pax7-DTA (Keller et al., 2004; Nishijo et al., 2009; Wu et al., 2006). Adult (4 months of age), female Pax7-DTA mice were administered either vehicle or tamoxifen (2 mg/day via IP injection) for five consecutive days followed by a two-week washout period. Immunohistochemical analysis of Pax7 expression in gastrocnemius muscles removed during SA surgery showed >90% ablation of satellite cells in tamoxifen-treated mice compared with vehicle-treated mice (Fig. 1A,B). FACS analysis confirmed the effective depletion of satellite cells, identified as the $CD34^+/\alpha7\text{-integrin}^+/CD31^-/CD45^-$ population (Fig. 1C) (Blanco-Bose et al., 2001; Rooney et al., 2009; Sacco et al., 2008). There was no change in immunohematopoietic ($CD45^+$) or endothelial ($CD31^+$) cell profiles, indicating that exposure to tamoxifen or the loss of satellite cells did not alter these cell populations in skeletal muscle (Fig.

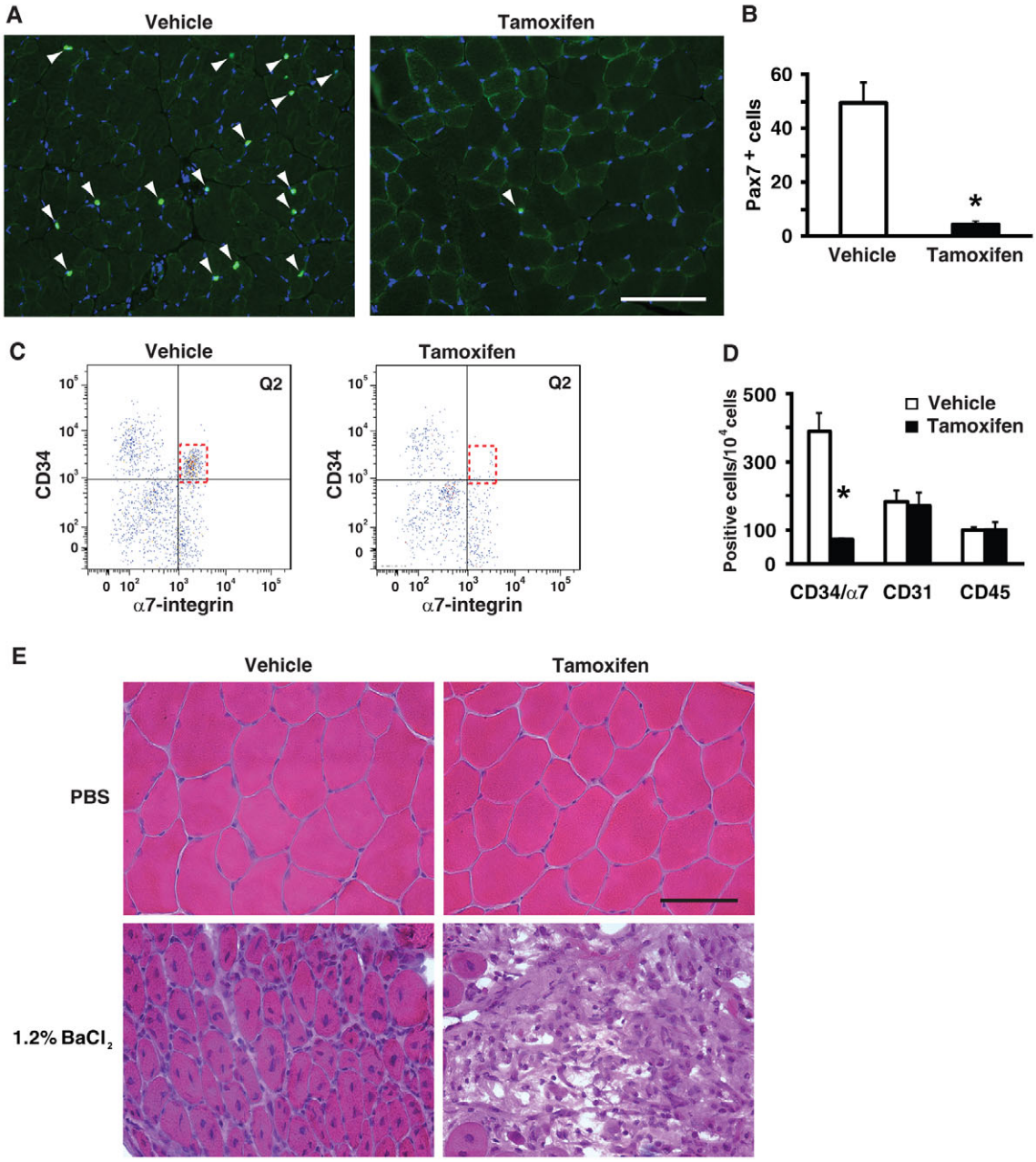

Fig. 1. Conditional ablation of satellite cells in adult skeletal muscle. (**A**) Pax7 immunohistochemistry (IHC) was performed on gastrocnemius muscle from vehicle and tamoxifen-treated Pax7-DTA mice to identify satellite cell nuclei (green). Sections were counterstained with DAPI (blue) and Pax7$^+$/DAPI$^+$ nuclei (white arrowhead) were counted. Scale bar: 100 μm. (**B**) Quantification of Pax7$^+$/DAPI$^+$ nuclei showed >90% (range 84-98%) ablation of satellite cells in tamoxifen-treated muscle compared with vehicle-treated muscle (vehicle, 49.2±5.0 vs tamoxifen, 4.70±0.5 satellite cells/muscle cross-section; *n*=10/treatment). (**C**) Fluorescence-activated cell sorting (FACS) analysis revealed depletion of CD34$^+$/α7-integrin$^+$/CD31$^-$/CD45$^-$ cells in tamoxifen-treated group relative to vehicle (compare red dotted box in Q2). (**D**) Quantification of FACS analysis showed >80% loss of satellite cells (CD34$^+$/α7-integrin$^+$/CD31$^-$/CD45$^-$) in tamoxifen-treated muscle relative to vehicle-treated muscle (vehicle, 392±52 vs tamoxifen, 70±5 cells/10,000 cells; *n*=4/treatment) with no change in immunohematopoietic (CD45$^+$) or endothelial (CD31$^+$) cell profiles. (**E**) The tibialis anterior muscle was severely damaged by 1.2% $BaCl_2$ injection and allowed to regenerate for seven days. Hematoxylin and Eosin (H&E) staining showed successful regeneration in vehicle-treated muscle, as indicated by distinct myofibers with centrally located nuclei, whereas tamoxifen-treated muscle depleted of satellite cells failed to regenerate. Scale bar: 50 μm. Values are presented as mean ± s.e.m. with significant difference (P<0.05) between vehicle and tamoxifen groups designated by an asterisk.

1C,D). As further confirmation that satellite cells had been significantly depleted, we examined muscle regeneration in muscle severely injured by $BaCl_2$ injection. Regeneration was significantly compromised in muscle depleted of satellite cells as indicated by the absence of distinct muscle fibers with central nuclei compared with vehicle-treated muscle (Fig. 1E). These results demonstrate that the Pax7-DTA strain provided an effective strategy to substantially deplete satellite cells in adult skeletal muscle.

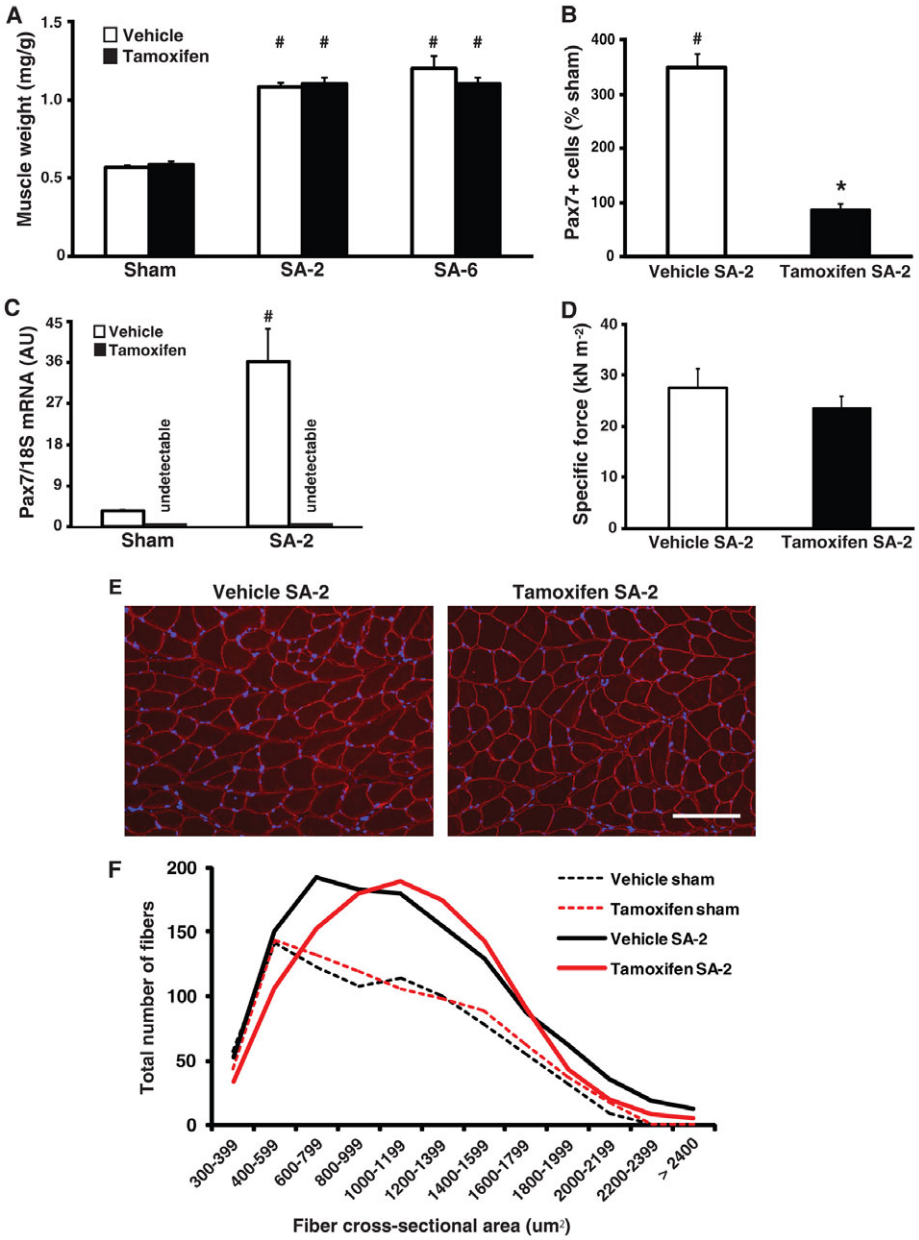

Fig. 2. Robust hypertrophy in satellite cell-depleted plantaris muscle. (**A**) Normalized muscle weight (muscle weight/body weight, mg/g) increased approximately twofold in both SA-2 and SA-6 groups relative to their respective sham control. (**B**) In response to SA-2, Pax7 immunohistochemistry (IHC) showed that satellite cell abundance, relative to sham control, increased by 360% in vehicle-treated muscle but remained unchanged in tamoxifen-treated muscle. (**C**) As measured by real-time RT PCR, *Pax7* mRNA expression increased by ~15-fold in vehicle SA-2 muscle relative to sham control but was undetectable in tamoxifen sham and SA-2 groups, consistent with ablation of satellite cells. (**D**) Single fiber mechanics revealed no difference in maximum isometric force normalized to fiber cross-sectional area (specific force) between SA-2 groups (n=12/group). (**E**) Dystrophin IHC (red) to visualize the cell membrane showed no difference between SA-2 groups in gross fiber morphology. Scale bar:100 μm. (**F**) Line graph of fiber cross-sectional area distribution shows a rightward shift in SA-2 groups relative to respective sham controls, indicating a significant increase in the number of fibers with cross-sectional area of 600-1400 μm^2 (see Fig. S2E in the supplementary material for bar graph). Values are presented as mean ± s.e.m. with significant difference (P<0.05) between sham and SA-2 groups indicated by a hash and significant difference between SA-2 groups indicated by an asterisk.

Satellite cell-depleted muscle fibers undergo hypertrophy

Two weeks after synergist ablation (SA-2), satellite cell-depleted muscle (tamoxifen SA-2) showed the same twofold increase in plantaris muscle weight as the vehicle SA-2 group (Fig. 2A). Moreover, the increased muscle mass in response to SA was maintained until 6 weeks after synergist ablation (SA-6, the longest time point examined) with no difference in muscle weight between vehicle and tamoxifen SA-6 groups (Fig. 2A). Pax7 immunohistochemistry indicated that the abundance of satellite cells in the hypertrophied plantaris muscle increased by 360% in the vehicle SA-2 group but remained unchanged in the tamoxifen SA-2 group relative to their respective sham control groups (Fig. 2B and see Fig. S2A in the supplementary material). In agreement with this finding, *Pax7* transcript levels increased 15-fold in vehicle SA-2 but remained undetectable in both tamoxifen sham and SA-2 groups (see Fig. S1C in the supplementary material). Functional analysis performed on single muscle fibers showed no difference between SA-2 groups for a number of different parameters, including maximum isometric force normalized to fiber cross-sectional area (specific force) (Fig. 2C), k_{tr} in maximally activating solution (maximal rate of cross-bridge cycling), pCa_{50} (Ca^{2+} concentration required for half-maximal activation) and n (Hill coefficient, indicative of the cooperativity of the contractile apparatus) (Fig. S2B-D in the supplementary material). Collectively, these results demonstrate that the hypertrophic growth of satellite cell-depleted muscle was functionally no different from the vehicle SA-2 group.

Dystrophin immunohistochemistry of SA-2 cryosections revealed no difference in the gross morphology of muscle fibers between vehicle- and tamoxifen-treated SA-2 groups (Fig. 2E). Consistent with the increase in muscle weight observed in both SA-2 groups was a rightward shift in the fiber size distribution, reflecting an increase in the number of large fibers, particularly

fibers with cross-sectional area of 600-1400 μm^2 (Fig. 2F and see Fig. S2E in the supplementary material). Muscle fiber hypertrophy in both vehicle- and tamoxifen-treated SA-2 groups was accompanied by comparable muscle protein concentrations and an increase in total RNA (see Fig. S2F,G in the supplementary material), as well as an increase in activation of the Akt/mTOR signaling pathway, which is known to have a central role in skeletal muscle growth by enhancing protein synthesis through activation of downstream targets (Bodine et al., 2001). Phosphorylation of Akt (T308) and p70^{S6K1} (T389) was elevated more than twofold in both SA-2 groups (see Fig. S2H,I in the supplementary material), suggesting that the increase in anabolic signaling in response to mechanical overload was not dependent on satellite cells.

Regenerative process is independent of muscle hypertrophy

The mechanical overload placed on the plantaris muscle from synergist ablation is associated with the appearance of small fibers which are thought to be formed de novo from satellite cells at sites of muscle injury (McCormick and Schultz, 1992; Tamaki et al., 1996). Although the distribution of large, hypertrophied fibers was not affected by the loss of satellite cells, there was an ~8-fold increase in the total number of small fibers (cross-sectional area <300 μm^2) in the vehicle SA-2 group that was significantly reduced in the tamoxifen SA-2 group relative to respective sham control groups (Fig. 3A). Post-hoc analysis showed a significant correlation (r=0.68, P=0.004) between the number of residual satellite cells and the number of de novo fibers. We next quantified the number of fibers that expressed embryonic myosin heavy chain and had centrally located nuclei: two hallmarks of newly regenerating fibers. Approximately 30% of fibers in the vehicle SA-2 group expressed embryonic myosin or had centrally located nuclei, whereas less than 7% and 10% of fibers in satellite cell-depleted SA-2 muscle were positive for embryonic myosin or contained central nuclei, respectively (Fig. 3B-D). These results suggest that the regenerative process associated with this model of muscle growth was significantly blunted in muscle depleted of satellite cells. Together, these findings indicate that muscle fiber hyperplasia and regeneration are distinct from fiber hypertrophy with only the former two processes requiring satellite cells.

Expansion of myonuclear domain in satellite cell-depleted muscle hypertrophy

To maintain the ratio of myonuclei to cytoplasmic volume, i.e. the myonuclear domain, the number of myonuclei usually increases during hypertrophy, presumably through the fusion of satellite cells into the fiber. To determine whether myonuclear abundance increased in response to SA-2, we quantified the total number of myonuclei for the entire muscle cross-sectional area; myonuclei were identified as DAPI$^+$ nuclei residing within the muscle fiber, which was delineated by dystrophin immunoreactivity (see Fig. S3A in the supplementary material). The number of myonuclei per fiber significantly increased by 63% in the vehicle-treated SA-2 group but remained unchanged in the satellite cell depleted SA-2 group relative to their respective sham control groups (Fig. 4A). To quantify the myonuclear domain size in fibers, we counted DAPI-stained myonuclei of fixed single fibers from vehicle- and tamoxifen-treated SA-2 groups (see Fig. S3B in the supplementary material). The myonuclear domain of the tamoxifen SA-2 group increased by 32% in comparison with the vehicle SA-2 group, in agreement with the diminished incorporation of satellite cells in the tamoxifen SA-2 group (Fig. 4B). The increased myonuclear domain in tamoxifen SA-2 fibers was accompanied by a 17% increase in the size of individual myonuclei (see Fig. S3C in the supplementary material).

Growth response is independent of satellite cell abundance

To monitor directly myonuclear accretion, we quantified the number of myonuclei that had incorporated BrdU, the presumption being that such nuclei are derived from satellite cells that have replicated and then subsequently fused to the growing fiber (Schiaffino et al., 1976). BrdU was administered via drinking water (0.8 mg/ml) throughout the entire SA-2 period. Immunohistochemistry using BrdU and dystrophin antibodies showed that 27% of fibers in the vehicle SA-2 group contained a BrdU$^+$ myonucleus, whereas ~6% of fibers in the tamoxifen SA-2 group were BrdU$^+$ (Fig. 4C,D). The paucity of BrdU$^+$ muscle fibers in the tamoxifen SA-2 group provides further support for the finding that adult skeletal muscle hypertrophy does not require satellite cells or any other potentially proliferative cells. In fact, post-hoc analysis revealed no correlation between satellite cell number and growth response (r=0.241, P=0.254, Fig. 4E). Figure 4E also shows that there is no apparent threshold in the satellite cell number required to sustain growth, as muscle with <2% of its satellite cells hypertrophied to the same degree as muscle with 100% of its satellite cells. Thus, although satellite cell number is normally correlated with myonuclear number during hypertrophy (see Fig. S4 in the supplementary material), robust hypertrophy does not require myonuclear accretion.

DISCUSSION

The most significant finding from this study is that satellite cells are not required for skeletal muscle fiber hypertrophy; however, satellite cells are necessary for both the formation of new fibers and fiber regeneration. Given that new fibers and regeneration represent a minor component of the hypertrophic response, satellite cell-depleted muscle showed the same overall increase in muscle mass as vehicle-treated control muscle following two weeks of overload. The increase in fiber cross-sectional area in satellite cell-depleted muscle occurred independently of myonuclear accretion, resulting in a significant expansion of the myonuclear domain. Despite the greater myonuclear domain, satellite cell-depleted muscle was able to sustain the hypertrophic state for six weeks (the longest time point examined). Although we did not identify a compensatory mechanism enabling fiber growth without satellite cell participation, such as an increase in Akt/mTOR signaling, we did find an increase in the size of myonuclei in satellite cell-depleted muscle, suggesting an alteration in gene transcription as a result of chromatin reorganization (Brandt et al., 2006). It will be of great interest to determine in a future study whether satellite cell ablation leads to a compensatory change in gene expression that allows for the maintenance of a larger fiber size with an expanded myonuclear domain.

The development of the Pax7-DTA strain represents a significant improvement in the ability to ablate satellite cells in adult skeletal muscle, both in terms of specificity and effectiveness. In previous studies examining the necessity of satellite cells in muscle hypertrophy, γ-irradiation was most often used to ablate satellite cells (Adams et al., 2002; Phelan and Gonyea, 1997; Rosenblatt and Parry, 1992; Rosenblatt and Parry, 1993; Rosenblatt et al., 1994). These studies consistently showed that following γ-irradiation the hypertrophic response was either blunted or completely prevented, thus giving rise to the general consensus that satellite cells are required for muscle hypertrophy. Unfortunately, at the time these studies were performed, there was not yet an

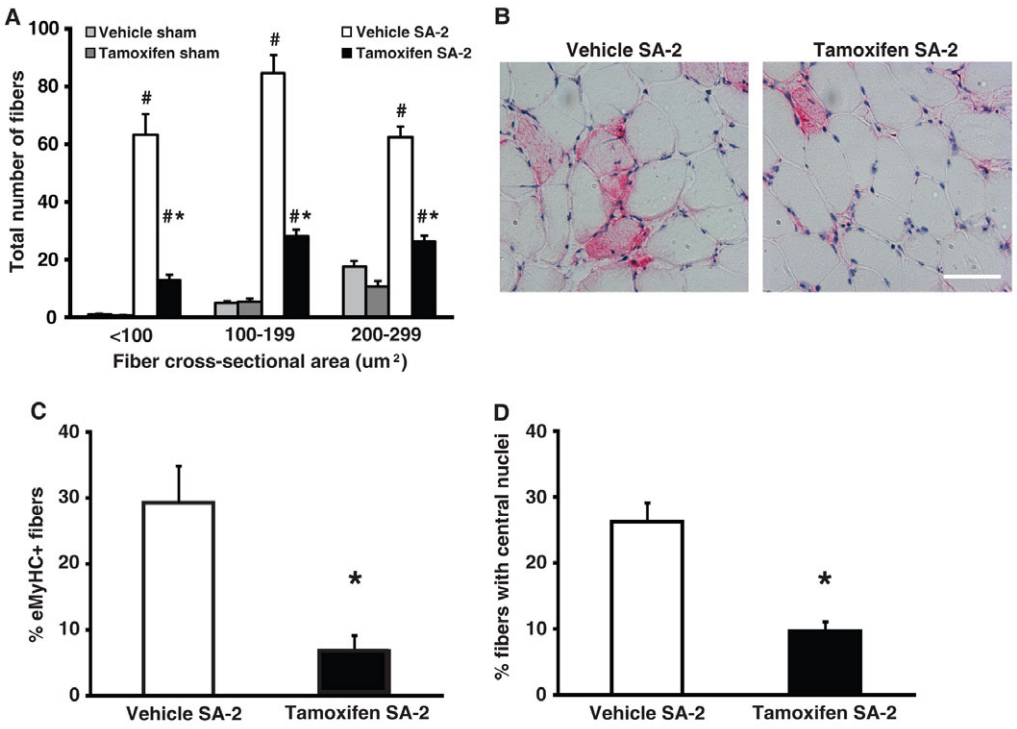

Fig. 3. Regeneration is blunted in satellite cell-depleted plantaris muscle. (**A**) The total number of small fibers (<300 μm^2) increased by approximately eightfold in vehicle SA-2 group but was significantly reduced in tamoxifen SA-2 relative to respective sham control (*n*=6-8/group). (**B**,**C**) Embryonic myosin expression (pink) was observed in 29% of vehicle SA-2 fibers and was significantly reduced to 7% of the fibers in tamoxifen SA-2 (*n*=4-5/group). Scale bar: 50 μm. (**D**) The number of fibers with centrally located nuclei was reduced from 26% in vehicle SA-2 to 10% in tamoxifen SA-2 (*n*=4-5/group). Values are presented as mean ± s.e.m. with significant difference (*P*<0.05) between sham and SA-2 groups indicated by a hash and significant difference between SA-2 groups indicated by an asterisk.

established method for reliably identifying satellite cells so it was not possible to assess directly the effectiveness of satellite cell ablation by γ-irradiation. A further limitation of these studies was the inability of γ-irradiation to ablate satellite cells specifically, thus opening up the real possibility that other cells important for hypertrophy were also adversely affected. Collectively, these methodological limitations call into question the conclusion that satellite cells are required for hypertrophy and emphasize the need for a more specific method of ablating satellite cells in adult muscle. The results from this study clearly show that the Pax7-DTA strain allows for >90% ablation of satellite cells in mature muscle. This high degree of effectiveness in cell ablation is similar to the 70-90% cell ablation reported in other cell populations using the DTA system (Arnold et al., 2007; Nir et al., 2007; Ohnmacht et al., 2009). Moreover, given that the murine genome does not harbor a DTA receptor, there is no collateral damage to either neighboring or distant cells as the satellite cells undergo apoptosis upon exposure to DTA. The finding from FACS analysis that neither immunohematopoietic (CD45$^+$) nor endothelial (CD31$^+$) cell profiles were altered is consistent with this idea and highlights the specificity of the system. Beyond the findings of this study, the Pax7-DTA strain will be an invaluable resource for exploring the role of satellite cells in other aspects of skeletal muscle biology, such as re-growth following muscle atrophy and the maintenance of muscle structure and function with age.

The ability to specifically ablate satellite cells in mature muscle allowed us to revisit and rigorously test the hypothesis that satellite cells are necessary for skeletal muscle hypertrophy. We found that depletion of satellite cells did not prevent or blunt the hypertrophic response in terms of muscle mass or fiber cross-sectional area, demonstrating that satellite cells were not necessary for hypertrophy. This unexpected finding goes against established dogma in the field and suggests that the use of γ-irradiation to ablate satellite cells also adversely affected another cell population(s) that, in combination with satellite cells, was needed for hypertrophy (Adams et al., 2002; Phelan and Gonyea, 1997; Rosenblatt and Parry, 1992; Rosenblatt and Parry, 1993; Rosenblatt et al., 1994). An alternative explanation for our finding is that the growth stimulus provided by SA was insufficient and was below some threshold requiring satellite cells, resulting in a false-negative, type II error. We think that this is an unlikely possibility given that SA has been shown to induce a maximal hypertrophic response that, in our hands, resulted in a twofold increase in muscle mass within two weeks (Tamaki et al., 2009a). The significant increase in Pax7$^+$ cells, myonuclei per fiber and BrdU$^+$ positive myonuclei in the vehicle-treated group are in agreement with previous studies and support the view that satellite cells are involved in the hypertrophic response induced by SA (Akiho et al., 2010; Ishido et al., 2009). The significant number of myonuclei that were BrdU$^+$ in the vehicle SA2 group was consistent with an earlier study by Westerkamp and Gordon (Westerkamp and Gordon, 2005) that reported that ~25% of myonuclei in rat plantaris muscle were BrdU$^+$ following SA (Westerkamp and Gordon, 2005). Thus, although satellite cells appear to be involved in muscle hypertrophy under normal circumstances, our findings indicate that they are not necessary.

The finding that muscle can hypertrophy independently of satellite cell participation is not without precedent. Specifically, it was reported that the muscle hypertrophy resulting from myostatin inactivation or overexpression of Akt occurred without the recruitment of satellite cells (Amthor et al., 2009; Blaauw et al., 2009). More recently, Raffaello and colleagues (Raffaello et al., 2010) showed that overexpression of the transcription factor JunB increased mean cross-sectional area by ~40% and did not involve satellite cells, as assessed by BrdU labeling of myonuclei (Raffaello et al., 2010). Consistent with these studies, we found, in satellite cell-depleted muscle undergoing hypertrophy, no change in the number of myonuclei per fiber, which was accompanied by a dramatic reduction (~80%) in BrdU$^+$ myonuclei. As a consequence, the size of the myonuclear domain in satellite cell-depleted fibers increased by 32%. These findings indicate that the myonuclei within satellite

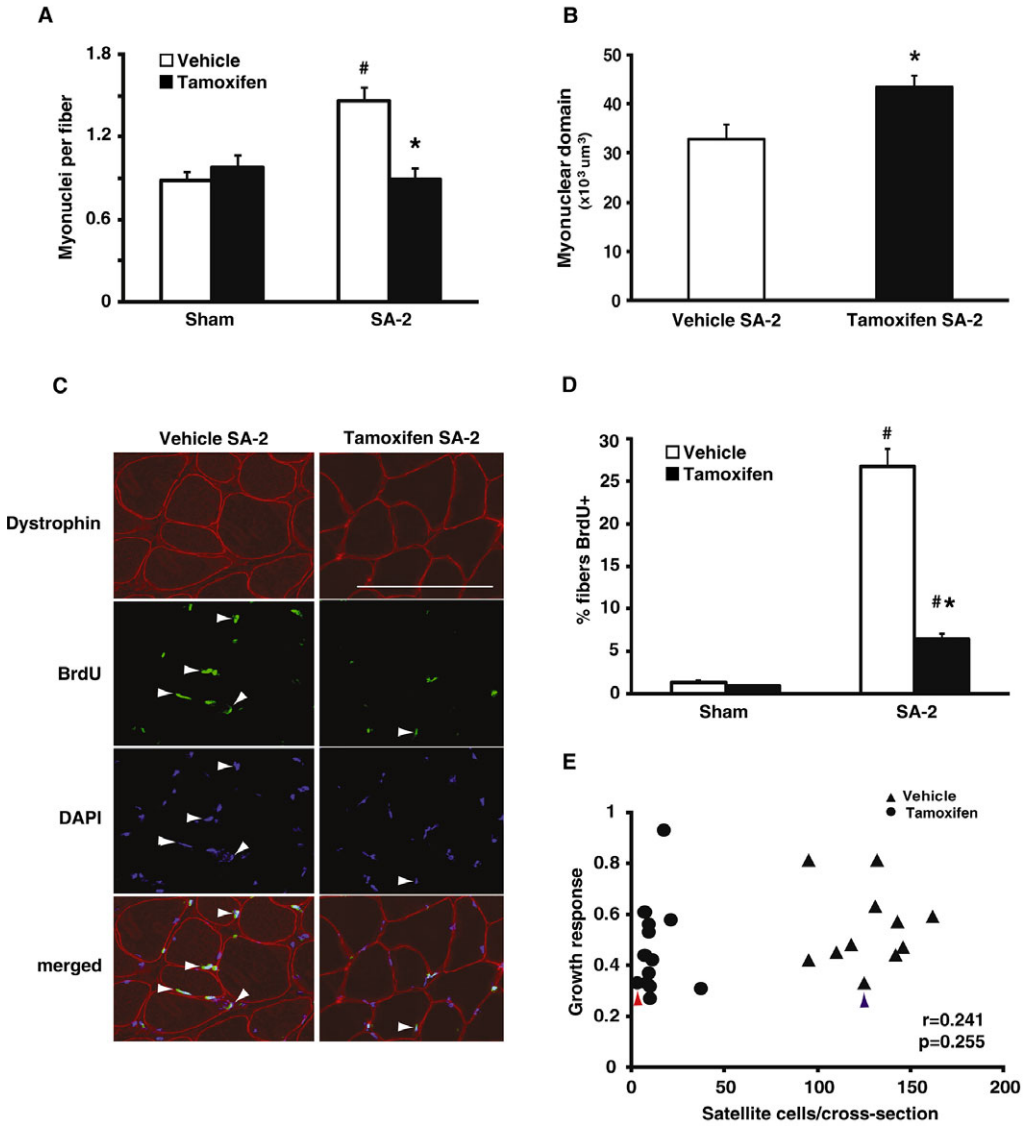

Fig. 4. Skeletal muscle hypertrophy is independent of myonuclear accretion. (**A**) Dystrophin immunohistochemistry (IHC) and DAPI staining were performed and DAPI$^+$ nuclei residing within the dystrophin antibody-stained sarcolemma were counted as myonuclei. The number of myonuclei increased by 63% in vehicle-treated SA-2 but remained unchanged in tamoxifen SA-2 relative to respective sham control (n=8/group). (**B**) DAPI$^+$ nuclei were counted in fixed single fibers isolated from vehicle- and tamoxifen-treated SA-2 muscles and myonuclear domain size was calculated. Myonuclear domain increased by 32% in tamoxifen SA-2 fibers compared with fibers isolated from vehicle-treated muscle. (**C**) Location of nuclei that had incorporated BrdU was determined in vehicle- and tamoxifen-treated SA-2 muscle sections by double IHC with dystrophin (red) and BrdU (green) antibodies and DAPI staining (blue). BrdU$^+$/DAPI$^+$ myonuclei residing within the sarcolemma (white arrowheads) were counted. Scale bar: 50 μm. (**D**) Nearly 30% of muscle fibers contained a BrdU$^+$ nucleus in vehicle SA-2,compared with ~1% in sham control, which was reduced significantly to 6% in tamoxifen SA-2 (n=4/group). (**E**) There was no correlation (r=0.241, P=0.255) between satellite cell abundance and growth response (change in normalized muscle weight in response to synergist ablation) as highlighted by the similar growth response in muscle in which 98% of the satellite cells have been ablated (solid circle with red arrowhead) and muscle with all of its satellite cells present (solid triangle with blue arrowhead). Values are presented as mean ± s.e.m. with significant difference (P<0.05) between sham and SA-2 groups indicated by a hash and significant difference between SA-2 groups indicated by an asterisk.

cell-depleted muscle possess the intrinsic capacity to ‘oversee’ a larger cytoplasmic volume, though the mechanism allowing for this adjustment remains completely unknown. The larger myonuclear size in hypertrophied satellite cell-depleted fibers is similar to what has been reported in growing yeast, in which nuclei adjust their size to maintain a roughly constant ratio between nuclear and cell volume, termed the ‘karyoplasmic ratio’ (Jorgensen et al., 2007; Neumann and Nurse, 2007).

Given that we were unable to ablate all the satellite cells, one possible explanation for our findings is that the remaining ~10% of satellite cells were sufficient to support the hypertrophic growth. This scenario proposes that there exists a minimal threshold for the number of satellite cells capable of supporting a full growth response, and that if the number falls below that threshold, the ability to hypertrophy would be impaired. To test this scenario, we plotted the growth response (i.e. change in the normalized muscle

weight) against satellite cell abundance for both SA-2 groups. This post-hoc analysis revealed no correlation between the abundance of satellite cells and the magnitude of the growth response; muscle that had only 2% of their satellite cells were still capable of mounting a full hypertrophic response. By contrast, we did find a significant correlation between the number of myonuclei and satellite cell abundance.

Another possible explanation for our findings is that some other progenitor cell population known to exist in adult muscle compensated for the loss of satellite cells (for a review, see Tedesco et al., 2010). This possibility seems unlikely as we did not see an increase in the number of myonuclei per fiber, indicating, regardless of cell identity, that few nuclei were being incorporated to the growing fibers in satellite cell-depleted muscle. Single fiber analysis and BrdU incorporation experiments confirmed this finding and provide strong evidence that no other cell population was substituting for satellite cells during muscle fiber hypertrophy.

The use of SA to induce muscle hypertrophy provided the opportunity to determine whether satellite cells are necessary for the formation of new fibers. The de novo formation of small, immature fibers has been generally considered to be part of a regenerative process that is satellite cell-dependent, though this viewpoint has never been tested directly (Snow and Chortkoff, 1987; Tamaki et al., 1996). The eightfold increase in the number of small fibers (<300 μm) in the vehicle SA-2 group was significantly reduced in satellite cell-depleted muscle subjected to SA. This finding supports the earlier proposition and represents the first evidence that the de novo formation of these small fibers requires satellite cells. The loss of small fibers in tamoxifen-treated muscle had a negligible effect on the overall hypertrophic response, given that these fibers account for <0.25% of the total cross-sectional area of the muscle. Consistent with the notion that small fiber formation is part of a regenerative process, we also observed a significant reduction in the number of fibers that expressed embryonic myosin and had centrally located nuclei in SA-2 satellite cell-depleted muscle. The failure of muscle fiber regeneration following severe muscle damage induced by $BaCl_2$ exposure confirmed the absolute necessity of satellite cells in the process of muscle regeneration.

The finding that hypertrophy of existing muscle fibers and muscle regeneration are mechanistically distinct has important clinical implications. Historically, it has been assumed that muscle hypertrophy required muscle damage and subsequent satellite cell activation to initiate the growth response. The findings from the current study indicate that fiber hypertrophy and regeneration from injury are two distinct processes or, at least, that they can be mechanistically uncoupled. If fiber hypertrophy does occur independently of muscle injury, as our data suggest, then exercise protocols designed to promote muscle growth should aim to minimize muscle damage and maximize intracellular anabolic processes (Burd et al., 2010; Flann et al., 2011). This might be particularly important for populations, such as the elderly, in which satellite cell activity is compromised.

Acknowledgements
This work was supported by grants from NIH to C.A.P. (AG020941 and AG034453), C.A.P. and J.J.M. (AR060701), K.S.C. (HL090749) and K.A.E. (AR045617). The authors would like to thank Katherine Baumgarner and Edgardo Dimayuga for excellent technical assistance and Jonah Lee for helpful discussion. Deposited in PMC for release after 12 months.

Competing interests statement
The authors declare no competing financial interests.

Supplementary material
Supplementary material for this article is available at
http://dev.biologists.org/lookup/suppl/doi:10.1242/dev.068858/-/DC1

References
Adams, G. R., Caiozzo, V. J., Haddad, F. and Baldwin, K. M. (2002). Cellular and molecular responses to increased skeletal muscle loading after irradiation. *Am. J. Physiol. Cell Physiol.* **283**, C1182-C1195.
Akiho, M., Nakashima, H., Sakata, M., Yamasa, Y., Yamaguchi, A. and Sakuma, K. (2010). Expression profile of Notch-1 in mechanically overloaded plantaris muscle of mice. *Life Sci.* **86**, 59-65.
Amthor, H., Otto, A., Vulin, A., Rochat, A., Dumonceaux, J., Garcia, L., Mouisel, E., Hourde, C., Macharia, R., Friedrichs, M. et al. (2009). Muscle hypertrophy driven by myostatin blockade does not require stem/precursor-cell activity. *Proc. Natl. Acad. Sci. USA* **106**, 7479-7484.
Arnold, L., Henry, A., Poron, F., Baba-Amer, Y., van Rooijen, N., Plonquet, A., Gherardi, R. K. and Chazaud, B. (2007). Inflammatory monocytes recruited after skeletal muscle injury switch into antiinflammatory macrophages to support myogenesis. *J. Exp. Med.* **204**, 1057-1069.
Blaauw, B., Canato, M., Agatea, L., Toniolo, L., Mammucari, C., Masiero, E., Abraham, R., Sandri, M., Schiaffino, S. and Reggiani, C. (2009). Inducible activation of Akt increases skeletal muscle mass and force without satellite cell activation. *FASEB J.* **23**, 3896-3905.
Blanco-Bose, W. E., Yao, C. C., Kramer, R. H. and Blau, H. M. (2001). Purification of mouse primary myoblasts based on alpha 7 integrin expression. *Exp. Cell Res.* **265**, 212-220.
Bodine, S. C., Stitt, T. N., Gonzalez, M., Kline, W. O., Stover, G. L., Bauerlein, R., Zlotchenko, E., Scrimgeour, A., Lawrence, J. C., Glass, D. J. et al. (2001). Akt/mTOR pathway is a crucial regulator of skeletal muscle hypertrophy and can prevent muscle atrophy in vivo. *Nat. Cell Biol.* **3**, 1014-1019.
Brack, A. S., Bildsoe, H. and Hughes, S. M. (2005). Evidence that satellite cell decrement contributes to preferential decline in nuclear number from large fibres during murine age-related muscle atrophy. *J. Cell Sci.* **118**, 4813-4821.
Brandt, A., Papagiannouli, F., Wagner, N., Wilsch-Brauninger, M., Braun, M., Furlong, E. E., Loserth, S., Wenzl, C., Pilot, F., Vogt, N. et al. (2006). Developmental control of nuclear size and shape by Kugelkern and Kurzkern. *Curr. Biol.* **16**, 543-552.
Bruusgaard, J. C., Johansen, I. B., Egner, I. M., Rana, Z. A. and Gundersen, K. (2010). Myonuclei acquired by overload exercise precede hypertrophy and are not lost on detraining. *Proc. Natl. Acad. Sci. USA* **107**, 15111-15116.
Burd, N. A., West, D. W., Staples, A. W., Atherton, P. J., Baker, J. M., Moore, D. R., Holwerda, A. M., Parise, G., Rennie, M. J., Baker, S. K. et al. (2010). Low-load high volume resistance exercise stimulates muscle protein synthesis more than high-load low volume resistance exercise in young men. *PLoS ONE* **5**, e12033.
Campbell, K. S. (2006). Tension recovery in permeabilized rat soleus muscle fibers after rapid shortening and restretch. *Biophys. J.* **90**, 1288-1294.
Cheek, D. B., Powell, G. K. and Scott, R. E. (1965). Growth of muscle mass and skeletal collagen in the rat. I. Normal growth. *Bull. Johns Hopkins Hosp.* **116**, 378-387.
Collins, C. A., Olsen, I., Zammit, P. S., Heslop, L., Petrie, A., Partridge, T. A. and Morgan, J. E. (2005). Stem cell function, self-renewal, and behavioral heterogeneity of cells from the adult muscle satellite cell niche. *Cell* **122**, 289-301.
Flann, K. L., Lastayo, P. C., McClain, D. A., Hazel, M. and Lindstedt, S. L. (2011). Muscle damage and muscle remodeling: no pain, no gain? *J. Exp. Biol.* **214**, 674-679.
Fleckman, P., Bailyn, R. S. and Kaufman, S. (1978). Effects of the inhibition of DNA synthesis on hypertrophying skeletal muscle. *J. Biol. Chem.* **253**, 3320-3327.
Fortado, C. M. and Barnett, J. G. (1985). Effects of inhibiting DNA synthesis with hydroxyurea on stretch-induced skeletal muscle growth. *Exp. Neurol.* **87**, 487-494.
Gordon, S. E., Davis, B. S., Carlson, C. J. and Booth, F. W. (2001). ANG II is required for optimal overload-induced skeletal muscle hypertrophy. *Am. J. Physiol. Endocrinol. Metab.* **280**, E150-E159.
Hidestrand, M., Richards-Malcolm, S., Gurley, C. M., Nolen, G., Grimes, B., Waterstrat, A., Zant, G. V. and Peterson, C. A. (2008). Sca-1-expressing nonmyogenic cells contribute to fibrosis in aged skeletal muscle. *J. Gerontol. A Biol. Sci. Med. Sci.* **63**, 566-579.
Ishido, M., Uda, M., Kasuga, N. and Masuhara, M. (2009). The expression patterns of Pax7 in satellite cells during overload-induced rat adult skeletal muscle hypertrophy. *Acta Physiol.* **195**, 459-469.
Jorgensen, P., Edgington, N. P., Schneider, B. L., Rupes, I., Tyers, M. and Futcher, B. (2007). The size of the nucleus increases as yeast cells grow. *Mol. Biol. Cell* **18**, 3523-3532.
Keller, C., Hansen, M. S., Coffin, C. M. and Capecchi, M. R. (2004). Pax3:Fkhr interferes with embryonic Pax3 and Pax7 function: implications for alveolar rhabdomyosarcoma cell of origin. *Genes Dev.* **18**, 2608-2613.
Kuang, S. and Rudnicki, M. A. (2008). The emerging biology of satellite cells and their therapeutic potential. *Trends Mol. Med.* **14**, 82-91.
Lepper, C., Conway, S. J. and Fan, C. M. (2009). Adult satellite cells and embryonic muscle progenitors have distinct genetic requirements. *Nature* **460**, 627-631.

Mauro, A. (1961). Satellite cell of skeletal muscle fibers. *J. Biophys. Biochem. Cytol.* **9**, 493-495.
McCarthy, J. J. and Esser, K. A. (2007). Counterpoint: satellite cell addition is not obligatory for skeletal muscle hypertrophy. *J. Appl. Physiol.* **103**, 1100-1102; discussion 1102-1103.
McCormick, K. M. and Schultz, E. (1992). Mechanisms of nascent fiber formation during avian skeletal muscle hypertrophy. *Dev. Biol.* **150**, 319-334.
Mitchell, P. O. and Pavlath, G. K. (2001). A muscle precursor cell-dependent pathway contributes to muscle growth after atrophy. *Am. J. Physiol. Cell Physiol.* **281**, C1706-C1715.
Miyazaki, M., McCarthy, J. J., Fedele, M. J. and Esser, K. A. (2011). Early activation of mTORC1 signalling in response to mechanical overload is independent of phosphoinositide 3-kinase/Akt signalling. *J. Physiol.* **589**, 1831-1846.
Moss, F. P. and Leblond, C. P. (1970). Nature of dividing nuclei in skeletal muscle of growing rats. *J. Cell Biol.* **44**, 459-462.
Neumann, F. R. and Nurse, P. (2007). Nuclear size control in fission yeast. *J. Cell Biol.* **179**, 593-600.
Nir, T., Melton, D. A. and Dor, Y. (2007). Recovery from diabetes in mice by beta cell regeneration. *J. Clin. Invest.* **117**, 2553-2561.
Nishijo, K., Hosoyama, T., Bjornson, C. R., Schaffer, B. S., Prajapati, S. I., Bahadur, A. N., Hansen, M. S., Blandford, M. C., McCleish, A. T., Rubin, B. P. et al. (2009). Biomarker system for studying muscle, stem cells, and cancer in vivo. *FASEB J.* **23**, 2681-2690.
O'Connor, R. S. and Pavlath, G. K. (2007). Point:Counterpoint: Satellite cell addition is/is not obligatory for skeletal muscle hypertrophy. *J. Appl. Physiol.* **103**, 1099-1100.
O'Connor, R. S., Pavlath, G. K., McCarthy, J. J. and Esser, K. A. (2007). Last word on Point:Counterpoint: satellite cell addition is/is not obligatory for skeletal muscle hypertrophy. *J. Appl. Physiol.* **103**, 1107.
Ohnmacht, C., Pullner, A., King, S. B., Drexler, I., Meier, S., Brocker, T. and Voehringer, D. (2009). Constitutive ablation of dendritic cells breaks self-tolerance of CD4 T cells and results in spontaneous fatal autoimmunity. *J. Exp. Med.* **206**, 549-559.
Oustanina, S., Hause, G. and Braun, T. (2004). Pax7 directs postnatal renewal and propagation of myogenic satellite cells but not their specification. *EMBO J.* **23**, 3430-3439.
Phelan, J. N. and Gonyea, W. J. (1997). Effect of radiation on satellite cell activity and protein expression in overloaded mammalian skeletal muscle. *Anat. Rec.* **247**, 179-188.
Raffaello, A., Milan, G., Masiero, E., Carnio, S., Lee, D., Lanfranchi, G., Goldberg, A. L. and Sandri, M. (2010). JunB transcription factor maintains skeletal muscle mass and promotes hypertrophy. *J. Cell Biol.* **191**, 101-113.
Rooney, J. E., Gurpur, P. B., Yablonka-Reuveni, Z. and Burkin, D. J. (2009). Laminin-111 restores regenerative capacity in a mouse model for alpha7 integrin congenital myopathy. *Am. J. Pathol.* **174**, 256-264.
Rosenblatt, J. D. and Parry, D. J. (1992). Gamma irradiation prevents compensatory hypertrophy of overloaded mouse extensor digitorum longus muscle. *J. Appl. Physiol.* **73**, 2538-2543.
Rosenblatt, J. D. and Parry, D. J. (1993). Adaptation of rat extensor digitorum longus muscle to gamma irradiation and overload. *Pflugers Arch.* **423**, 255-264.
Rosenblatt, J. D., Yong, D. and Parry, D. J. (1994). Satellite cell activity is required for hypertrophy of overloaded adult rat muscle. *Muscle Nerve* **17**, 608-613.
Sacco, A., Doyonnas, R., Kraft, P., Vitorovic, S. and Blau, H. M. (2008). Self-renewal and expansion of single transplanted muscle stem cells. *Nature* **456**, 502-506.
Schiaffino, S., Bormioli, S. P. and Aloisi, M. (1976). The fate of newly formed satellite cells during compensatory muscle hypertrophy. *Virchows Arch. B Cell Pathol.* **21**, 113-118.
Seale, P., Sabourin, L. A., Girgis-Gabardo, A., Mansouri, A., Gruss, P. and Rudnicki, M. A. (2000). Pax7 is required for the specification of myogenic satellite cells. *Cell* **102**, 777-786.
Snow, M. H. (1990). Satellite cell response in rat soleus muscle undergoing hypertrophy due to surgical ablation of synergists. *Anat. Rec.* **227**, 437-446.
Snow, M. H. and Chortkoff, B. S. (1987). Frequency of bifurcated muscle fibers in hypertrophic rat soleus muscle. *Muscle Nerve* **10**, 312-317.
Tamaki, T., Akatsuka, A., Tokunaga, M., Uchiyama, S. and Shiraishi, T. (1996). Characteristics of compensatory hypertrophied muscle in the rat: I. Electron microscopic and immunohistochemical studies. *Anat. Rec.* **246**, 325-334.
Tamaki, T., Uchiyama, Y., Okada, Y., Tono, K., Nitta, M., Hoshi, A. and Akatsuka, A. (2009a). Anabolic-androgenic steroid does not enhance compensatory muscle hypertrophy but significantly diminish muscle damages in the rat surgical ablation model. *Histochem. Cell Biol.* **132**, 71-81.
Tamaki, T., Uchiyama, Y., Okada, Y., Tono, K., Nitta, M., Hoshi, A. and Akatsuka, A. (2009b). Multiple stimulations for muscle-nerve-blood vessel unit in compensatory hypertrophied skeletal muscle of rat surgical ablation model. *Histochem. Cell Biol.* **132**, 59-70.
Tedesco, F. S., Dellavalle, A., Diaz-Manera, J., Messina, G. and Cossu, G. (2010). Repairing skeletal muscle: regenerative potential of skeletal muscle stem cells. *J. Clin. Invest.* **120**, 11-19.
Timson, B. F. (1990). Evaluation of animal models for the study of exercise-induced muscle enlargement. *J. Appl. Physiol.* **69**, 1935-1945.
Tsika, R. W., Hauschka, S. D. and Gao, L. (1995). M-creatine kinase gene expression in mechanically overloaded skeletal muscle of transgenic mice. *Am. J. Physiol.* **269**, C665-C674.
Westerkamp, C. M. and Gordon, S. E. (2005). Angiotensin-converting enzyme inhibition attenuates myonuclear addition in overloaded slow-twitch skeletal muscle. *Am. J. Physiol. Regul. Integr. Comp. Physiol.* **289**, R1223-R1231.
Wu, S., Wu, Y. and Capecchi, M. R. (2006). Motoneurons and oligodendrocytes are sequentially generated from neural stem cells but do not appear to share common lineage-restricted progenitors in vivo. *Development* **133**, 581-590.
Zammit, P. S., Partridge, T. A. and Yablonka-Reuveni, Z. (2006). The skeletal muscle satellite cell: the stem cell that came in from the cold. *J. Histochem. Cytochem.* **54**, 1177-1191.